

Multi-instance Finger Knuckle Print Recognition based on Fusion of Local Features

Amine AMRAOUI^{1*}, Mounir AIT KERROUM², Youssef FAKHRI³
LaRI Laboratory, Faculty of Science, Ibn Tofail University, Kenitra, Morocco^{1,3}
LaRI Laboratory, ENCG, Ibn Tofail University, Kenitra, Morocco²

Abstract—Personal identity has become an important asset in today's digital world for any individual in society. Biometrics offers itself as a reliable and secure guarantor of our identities, so it has become essential to build efficient and robust recognition systems. In this orientation, we propose a fusion approach, which aims to optimally exploit the dividing block dimensions in the case of local methods to reduce similarities. We will use the compound local binary model (CLBP) for local features extraction, a robust operator descriptor that exploits both the sign and the inclination information of the differences between the center and the neighbor gray values. The reliability of the proposed approach was evaluated on the PolyU Finger Knuckle Print (FKP) database. We presented several experimental results that show the detailed path of our approach, explain the choices made for each step and illustrate the significant improvements compared to other existing recognition systems in the literature. The recognition rate of the proposed global approach is one of the highest among the other methods. Optimal final approach recognition rates vary between 99.70% and 100%.

Keywords—Biometrics; Finger Knuckle Print; local features; fusion; compound local binary pattern

I. INTRODUCTION

The security of personal identity has become a major asset in the development of the world we live in. This era has a wide spectrum of daily transactions that are in the billions, given the number of the world's population involved in the digital world and its applications. This digital world is committed to the development of many services, the main purpose of which is to facilitate this mass of interaction between the population and the services, and to ensure the efficiency of all the transactions that can be judging sensitive; such as finance and communication. These needs are generally linked to many risks, particularly security. The implementation of mechanisms and efficient applications to ensure personal identity has become important and urgent given the daily risks. To overcome these risks, the use of biometrics is an effective way to solve security difficulties in various fields and services [1].

During the last decades, several research works have been conducted to build reliable recognition systems. Researchers have exploited and experimented with various biometric modalities including face, voice, fingerprint, palm print, iris, [2-6], etc. Some types of these biometric descriptors show an intrusive nature [7]. It should be noted that the acceptance and ease of use of biometric identifiers play a key role in the success of recognition systems. To ensure these two points, the thinking of the researchers was drawn to the hand-based

descriptors. There is a lot of research and promising results in the literature on hand-based biometric modalities, e.g. hand [8], [9], palm print [10], [11], fingerprint [12], [13], and hand geometry [14], [15], which have been widely studied. These studies have allowed the construction of a large set of recognition systems to ensure the identity authentication function and which operate successfully in several areas.

The most common identification systems in the real world are based on the use of fingerprint recognition, moreover it is the most used system in the field of access control, the police etc. Moreover, the most reliable systems are based on the use of the iris as an identification modality. Except that, these two descriptors represent drawbacks, which can hinder their success, iris sensors represent high intrusiveness, which makes them not very acceptable by users and extraction of small unique features called minutiae from damaged fingerprints is difficult [16]. It is added to the two drawbacks cited, the fact that fingerprints are vulnerable to spoofing attacks which consist in the creation of biometric artefacts. Matsumoto et al. [17] found that gummy fingers were accepted with high recognition rates by the 11 different fingerprint systems they used. These forged fingerprints are easily achievable with readily available devices and materials. This vulnerability is due to the anatomical structure of the hand and the mechanisms of its movements; in fact, the use requires a contact surface between the hand bottom and the object used, this interaction will keep traces of fingerprints and palm prints on this object. To overcome this problem, one of the proposed solutions is to employ the back side of the hand. In recent years, researchers have observed that the skin pattern of the outer surface of the fingers, especially in the area around the phalangeal joint, has a rich texture due to the lines and folds of the skin. This texture shows a distinctive character given the uniqueness it represents; therefore the finger knuckle print can be used as a biometric descriptor [18], [19].

In the literature, researchers have begun their work to create recognition systems based on finger knuckle print FKP, with approaches based on the use of global characteristics such as: principal component analysis (PCA), independent component analysis (ICA) and linear discriminant analysis (LDA) [20]. Subspace analysis approaches are methods whose concept is suitable for large devices; they are rather effective for large areas such as facial recognition, which reduces their performance for systems that use descriptors with smaller surfaces such as FKP images [21]. Subsequently, researchers turned to multi-algorithm or multimodal approaches [22-24]. The mechanisms based on these approaches have shown

*Corresponding Author.

satisfactory results in the majority of cases. Based on this observation, we directed our work towards FKP recognition systems using local and not global characteristics, given the nature of the descriptor. Also, our orientation to ensure maximum reliability was to continue work towards the construction of a multi-instance biometric system, based on a reliable and robust extraction algorithm.

The response to these established expectations was the motivation we set ourselves to propose an efficient approach, which relies on the use of local characteristics to build a reliable multi-instance recognition system and which allows reducing the complexity of the calculations, as well as the implementation cost will be optimized. The proposed approach is based on the use of the compound local binary model (CLBP) [25] for the assurance of the local feature extraction phase. In this phase, we experimented and evaluated this method on several block sizes and also the nature of the block (square or rectangular), which is often neglected in other works, to produce optimal histograms and achieve the best possible results. The classification phase will be oriented towards classifiers based on the use of distances, this kind of classifiers can produce good results in the case of low resolution images, which we will use. We have opted for three variants of measurements: Euclidean distance, Jeffrey divergence and city block, which we will study their performance with our extracted characteristics and choose the most suitable to work in a real-time environment and produce effective results.

This paper is organized as follows: in Section 2, we will describe the proposed approach and the methods used. In Section 3, we will report and discuss the experimental results conducted on the PolyU FKP database [26] and finally, in Section 4, we will draw our conclusions.

II. PROPOSED APPROACH

The construction of recognition systems in the real world is based on several factors. The reliable recognition rates, the reduction of the calculation time and the robustness are decisive assets. In the approach we propose, we aim to satisfy these factors. This work is divided into three phases:

In the first phase, we will address two major points that will later be used to build our final system. The first point during this phase is to show that the recognition system based on local feature extraction with a compound local binary pattern (CLBP) can provide reliable results.

The second point concerns the matching phase, which is a very important step and can be costly in computation time. To satisfy this constraint, we will proceed with distance-based classifiers to reduce the computation time. We are going to test three classifiers during the first phase and take the most appropriate one in relation to the local extraction method used (recognition rate and computation time). The system used for this evaluation is shown in Fig. 1.

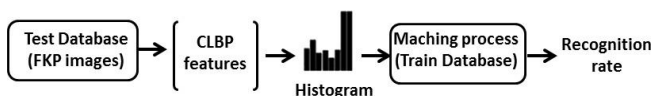


Fig. 1. FKP Recognition System Adopted for Evaluation.

During the second phase, we will proceed to an analysis and a comparison of the results obtained with other methods, in order to demonstrate the efficiency of the method to be used in our system.

In the end, the last phase consists in using the results and the conclusions obtained in the two previous phases to test the effectiveness of our global system, which is based on the concept of fusion at score level. The results obtained in the last phase will be analyzed and compared with phase 2. The proposed FKP recognition system is shown in Fig. 2.

A. Local Feature Extraction Process

Recognition systems generally satisfy two overriding conditions: high recognition rates and low computational cost. Note that the capture phase may be affected by environmental conditions. To overcome this problem, the local feature extraction phase will be ensured by a robust variant of Local Binary Patterns (LBP), this variant is called Compound Local Binary Patterns (CLBP) [25]. Ojala and Ai [27] introduced the local binary pattern method for the first time as an efficient method for feature extraction from images. The features extracted by this process have provided an efficient means for texture segmentation and classification.

The local binary pattern is recognized by a gray scale texture operator characterizing the local spatial structure of the image texture [28]. Given a central pixel in the image, a pattern code is calculated by comparing it to its neighbors. This procedure is illustrated in Fig. 3.

The LBP operator takes the form:

$$LBP(x_c, y_c) = \sum_{n=0}^7 2^n S(i_n - i_c) \tag{1}$$

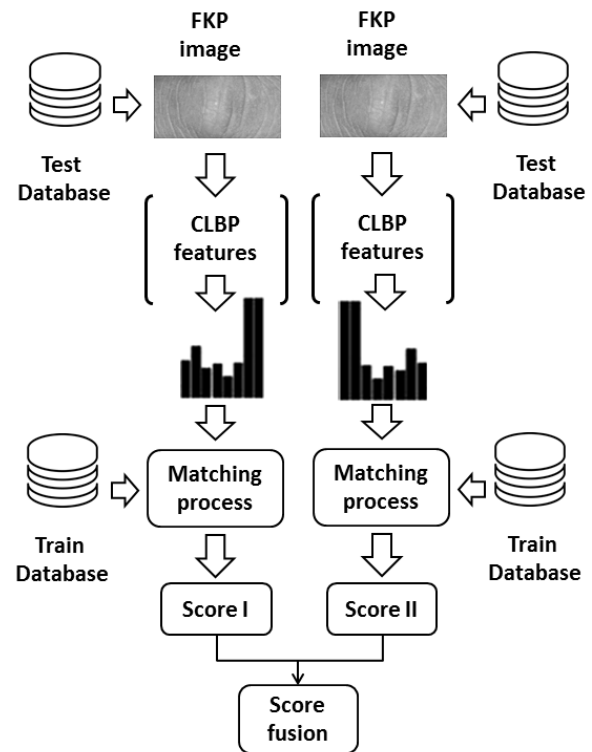


Fig. 2. The Proposed FKP Recognition System.

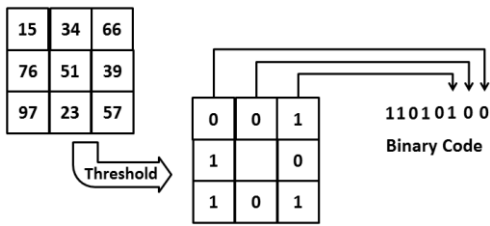


Fig. 3. Local Binary Pattern Operator.

where in this case n runs over the eight neighbors of the central pixel c , i_c and i_n are the gray-level values at c and n . Function $S(x)$ is shown below,

$$S(x) = \begin{cases} 1 & \text{if } x \geq 0 \\ 0 & \text{if } x < 0 \end{cases} \quad (2)$$

The LBP operator employs a process that relies solely on the use of the sign of the difference between two gray values, which often leads to a failure to generate binary codes consistent with the texture properties for local region. To overcome this problem, we will use an extension of this operator. This extension assigns a 2P bit code to the central pixel based on the gray values of the local neighborhood comprising P neighbors; this extension is the Compound Local Binary Pattern method (CLBP) [29]. The CLBP operator employs two bits for each neighbor in order to encode the sign as well as magnitude information of the difference between the center and the neighbor gray values, unlike the LBP that uses only one bit for each neighbor by representing the sign of the difference between the center and the corresponding neighbor gray values. In this case, the first bit is representing the sign of the difference between the center and the corresponding neighbor gray values as the basic LBP encoding. The second bit is for encoding the magnitude of the difference with respect to a threshold value, which is the average magnitude M_{avg} of the difference between the center and the neighbor gray values in the local neighborhood of interest. This CLBP operator chooses the value of 1 for the second bit if the magnitude of the difference between the center and the corresponding neighbor is greater than the threshold M_{avg} . Other way, it takes the value of 0. Thus, the indicator $s(x)$ of equation 2 is replaced by the following function:

$$s(i_p, i_c) = \begin{cases} 00 & i_p - i_c < 0, |i_p - i_c| \leq M_{avg} \\ 01 & i_p - i_c < 0, |i_p - i_c| > M_{avg} \\ 10 & i_p - i_c \geq 0, |i_p - i_c| \leq M_{avg} \\ 11 & \text{otherwise} \end{cases} \quad (3)$$

where i_c and i_p are the gray values of the central pixel and the neighbors, and the average magnitude of the difference between i_p and i_c in the local neighborhood is M_{avg} . The illustration of the CLBP operator is shown in the Fig. 4.

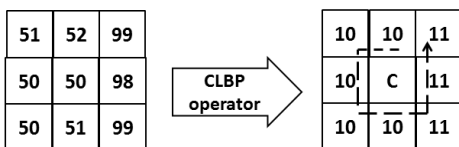


Fig. 4. Compound Local Binary Pattern Operator.

In Fig. 4, it can be observed that the CLBP operator discriminates the neighbors of the northeast, east and southeast directions because they have higher gray values than the other neighbors, thus producing a consistent local model.

B. Matching Process

Our choice of classifiers that can be used in our system was based on two important points. The first concerns the computation time, which is an important asset for the success of a recognition system, which directs us towards distance-based classifiers. The second point concerns the resolution of our images, which is not high, so we avoid classifiers such as SVM, which is rather oriented for high resolutions [30], [31]. Taking into account the guidelines already mentioned, we opted for a set that includes three distance-based classifiers, which we will experiment with the extraction method employed and see their performance for recognition rates generation. These classifiers are based on the Euclidean distance, Jeffrey Divergence and City-block.

The Euclidean distance is the most common distance metric used for low dimensional data sets, examines the root of square differences between the coordinates of a pair of objects. This is most generally known as the Pythagorean Theorem. For testing we used this classifier, for calculating the minimum distance between the test image and train image. Euclidean distance d is presented as follows:

$$d(x, y) = \sqrt{\sum_{i=1}^n (x_i - y_i)^2} \quad (4)$$

The Jeffrey divergence is a modification of the Kullback-Leibler (KL) divergence, if $P = (p_1, \dots, p_N)$ and $Q = (q_1, \dots, q_N)$ are two discrete distributions, the Jeffrey divergence between P and Q is defined as:

$$D(P, Q) = \sum_i (p_i \log \frac{p_i}{m_i} + q_i \log \frac{q_i}{m_i}) \quad (5)$$

$$\text{Where } m_i = \frac{(p_i + q_i)}{2}$$

The city-block distance classifier, Manhattan distance classifier, also called, rectilinear distance, L1 distance, L1 norm, Manhattan length. It represents the distance between points in a city road grid. It examines the absolute differences between the coordinates of a pair of objects as follows:

$$d(x, y) = \sum_{i=1}^n |x_i - y_i| \quad (6)$$

III. EXPERIMENTAL RESULT

In this section, we will proceed with various experiments to prove the reliability of the proposed recognition scheme. For a comparative evaluation of our recognition system, we will conduct experiments on the PolyU database [26]. This database is part of the databases, which can be described as referential databases in this field.

A. FKP PolyU Database

The PolyU FKP database is identified as a reference in biometrics research work (Fig. 5). This benchmark is used for evaluating the performance of the majority of FKP recognition systems that have been studied. The database construction was made thanks to the participation of 165 volunteers, including 40 women and 125 men. Among them, 143 individuals aged

between 20 and 30 years old and the rest between 30 and 50 years old. Two separate sessions have been designed to collect FKP images. During these two sessions, the volunteer is asked to provide six images for each of the right index finger, left index finger, right middle finger and left middle finger. All the original FKP images used have a resolution equal to 220x110. In the end, each subject is determined by $12 \times 4 = 48$ images, 12 FKP images of each finger. Thus, the database total is 7920 images from 660 fingers.

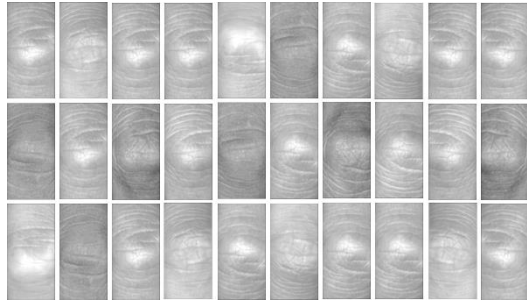


Fig. 5. Finger Knuckle Print PolyU Database.

B. Evaluation and Analysis of Results

In order to validate our recognition system, we have established an evaluation process divided into three different phases. The first step concerns a single finger knuckle print evaluation of our scheme, this step aims to determine the classifiers able to provide reliable results, and then we choose the most efficient ones. During this step, we will perform detailed experiments for each finger. The object of these experiments will be to determine the most suitable classifiers for our case study (recognition rate), the overall time taken by the matching phase for all the classes which are of the order of 165 classes, each class uses 6 test images which will be compared to 6×165 images = 990 images, we will call later in the experiments this computation time: Matching Process Time MPT. We will also introduce the division of the image into sub-images according to the type of resolution (square or rectangular) and conclude whether it is possible to introduce this kind of rectangular division, which is generally absent in the literature. In the second step, after having obtained the results and their analysis, we will proceed to a comparison with the other mechanisms already cited in the literature, which have used finger knuckle prints for the creation of recognition systems and conclude on the obtained performance. Finally, in the last part, we will use the directives obtained in our global approach, see its impact on performance and demonstrate the reliability of the proposed approach.

Single finger knuckle print evaluation in this first step, we will apply the same experimental protocol used by the others systems cited in literature. The 6 images captured during the first session are used to create the training database and the 6 images captured in the second session for the testing database. Therefore, for each volunteer, there are six training samples and six testing samples (Fig. 6). Our approach is based on local methods. The performance of scheme is evaluated with different sizes of sub images for each FKP image.

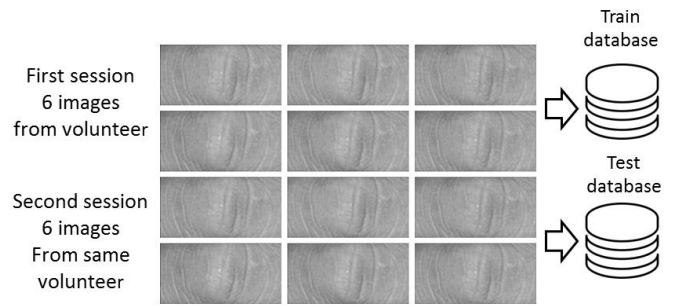


Fig. 6. Standard Protocol used for FKP Experiment.

We have categorized block sizes into three divisions: large division, medium division and small division. Large division is defined by two type of size block: 110x110 and 64x64, for medium size: 48x48 and 32x32 pixels, and for small size: 24x24 and 16x16. In order to increase Classification Process Performance of our approach, we have inspected many classifiers based on the squared Euclidean distance, the divergence of Jeffrey and City-Block. The recognition rates for each finger with the different divisions of sub-images are presented in the comparative Tables I, II, III, IV, V, VI, VII and VIII. This comparative evaluation is made with the intention of showing the most adaptive classifiers in our case.

1) *Result of experiment on left index finger:* The Table I shows the adequacy of classifiers based on distance city-Block and Jeffery divergence compared to the classifier based on Euclidean distance. The city-block classifier gives the best recognition rate value 98.18% for divisions (sub-images) of 16x16 pixels. We also notice that the Matching Process Time MPT increases proportionally with the decrease of the dividing block size. This observation is normal, since the smaller the block size, the more the number of sub-images increases (for image), and therefore the histogram of the image too. As we can also notice that even if the recognition rates can be equivalent between city-block and Jeffrey divergence, the MPT with the Jeffrey divergence classifier is much higher, we can cite the case of the 16x16 pixel block where the MPT for city block equal to 21.30s while that obtained with Jeffrey divergence equal to 852.96s.

It should be noted that these divisions (16x16, 24x24, 32x32, 48x48 and 64x64) are the most used in the literature. Nevertheless, we must not limit ourselves to this rule often used by researchers; we can extend the division with blocks of rectangular sub-images and not only square ones. In our case, we have an image whose size is 220x110 pixels; it would be wise to choose a division, which participates in an optimal construction of the histograms of each sub-image. In this sense to verify this proposal and based on the analysis of the optimal results obtained with blocks, which vary between 16x16 and 24x24 pixels and the shapes of the lines in the FKP images, we will extend the experiment to the 11x22 pixels blocks. This block division has exact multiples for the size of our FKP (220x110) images $11 \times 20 = 220$ pixels and $22 \times 5 = 110$ pixels, which gives for the division $(220 \times 110) \setminus (11 \times 22) = 100$ sub-images.

TABLE I. RECOGNITION RATE FOR LEFT INDEX WITH TYPICAL BLOCKS

		Table Recognition rate RR (Left index)		
Block size	RR/MPT	Euclidian distance	Jeffrey divergence	City-Block
110x110	RR	78,69%	88,79%	87,07%
	MPT	1,383645 s	22,262518	1,678907 s
64x64	RR	90,10%	94,75%	93,74%
	MPT	1,525478 s	73,938122 s	2,721189 s
48x48	RR	92,12%	95,35%	95,55%
	MPT	1,142311 s	96,140630 s	2,851411 s
32x32	RR	94,95%	96,86%	96,67%
	MPT	1,932484 s	273,279155 s	7,005333 s
24x24	RR	96,16%	97,37%	98,08%
	MPT	2,615035 s	422,307223 s	10,967445 s
16x16	RR	96,26%	97,98%	98,18%
	MPT	3,784349 s	852,959212 s	21,302479 s

TABLE II. RECOGNITION RATE FOR LEFT INDEX WITH RECTANGULAR BLOCK

		Table Recognition rate RR (Left index)		
Block size	RR/MPT	Euclidian distance	Jeffrey divergence	City-Block
11x22	RR	96,56%	97,98%	98,48%
	MPT	3,613546 s	877,053453 s	21,665596 s

In the Table II, we notice that the division of the image into sub-images with blocks size 11x22 pixels gives an optimal recognition rate with a value of 98.48%, this value rivals that obtained by the 16x16 block whose value is 98,18%. We are going to opt for this additional experience for the rest of the fingers (right Index, left middle and right middle).

2) *Result of experiment on right index finger:* In Table III, the obtained results affirm once again the adequacy of the resulting recognition rate with the classifiers based on the Jeffrey divergence and the City-block. We note that the value of the high recognition rate obtained is 98.48% with city block for a size block 24x24 pixels. As we mentioned before we are going to continue the complement of the experiment with the block whose size is 11x22 pixels. For MPT, we observe the same remark as before.

In the Table IV, we still notice the same remark and that the division of the image into sub-images with block of size 11x22 pixels gives optimal recognition rate with a value of 98.69%, this value remains equivalent or higher than that obtained by the 24x24 block whose value is 98.48%. It should be noted that even if we have equivalence in terms of recognition rates for the 11x22 pixels blocks with Jeffrey divergence and City-block, there remains the MPT factor, which gives a considerable advantage for City-block. The operation with Jeffrey divergence is more cost in computation time, MPT equal: 570, 16 s.

3) *Result of experiment on left middle finger:* Table V still shows the results superiority of the obtained recognition rates with the classifiers based on the Jeffrey and City-block divergence. We note that the value of the highest recognition rate is 99.29% with city-block for size 16x16 pixels. We will continue our experiments with the complement concerning the 11x22 pixels blocks.

TABLE III. RECOGNITION RATE FOR RIGHT INDEX WITH TYPICAL BLOCKS

		Table Recognition rate RR (Right index)		
Block size	RR/MPT	Euclidian distance	Jeffrey divergence	City-Block
110x110	RR	79,90%	90,80%	88,89%
	MPT	0,938604 s	14,560413 s	1,169245 s
64x64	RR	91,61%	96,57%	95,86%
	MPT	1,049516 s	47,949257 s	1,799466 s
48x48	RR	93,94%	97,37%	97,27%
	MPT	1,153916 s	94,779885 s	2,828075 s
32x32	RR	96,77%	97,88%	98,28%
	MPT	1,378431 s	175,976525 s	175,976525 s
24x24	RR	96,36%	98,18%	98,48%
	MPT	1,841294 s	286,073108 s	7,029212 s
16x16	RR	96,36%	97,88%	97,88%
	MPT	2,416625 s	554,749914 s	13,857284 s

TABLE IV. RECOGNITION RATE FOR RIGHT INDEX WITH RECTANGULAR BLOCK

		Table Recognition rate RR (Right index)		
Block size	RR/MPT	Euclidian distance	Jeffrey divergence	City-Block
11x22	RR	96,46%	98,69%	98,69%
	MPT	2,451808 s	570,162648 s	14,020781 s

TABLE V. RECOGNITION RATE FOR LEFT MIDDLE WITH TYPICAL BLOCKS

		Table Recognition rate RR (Left middle)		
Block size	RR/MPT	Euclidian distance	Jeffrey divergence	City-Block
110x110	RR	82,12%	91,41%	90,61%
	MPT	0,942734 s	14,488085 s	1,122162 s
64x64	RR	91,81%	95,86%	95,86%
	MPT	1,035171 s	47,818859 s	1,788124 s
48x48	RR	94,24%	97,07%	97,07%
	MPT	1,163299 s	95,044139 s	2,828460 s
32x32	RR	96,76%	97,68%	98,48%
	MPT	1,359258 s	175,401198 s	4,502957 s
24x24	RR	97,58%	98,59%	98,89%
	MPT	1,726323 s	287,939161 s	7,067663 s
16x16	RR	97,17%	98,89%	99,29%
	MPT	2,704647 s	550,270049 s	13,806499 s

TABLE VI. RECOGNITION RATE FOR LEFT MIDDLE WITH RECTANGULAR BLOCK

		Table Recognition rate RR (Left middle)		
Block size	RR/MPT	Euclidian distance	Jeffrey divergence	City-Block
11x22	RR	96,87%	98,99%	98,89%
	MPT	2,508779 s	569,049885 s	14,005159 s

The results obtained in the Table VI show that the division of the image into sub-images with 11x22 pixels always gives optimal recognition rates with a value of 98.89% in the case of city-block. This value still remains near to that obtained by the 16x16 pixels division, which has a value equal to 99.29% and equal to that obtained by the 24x24 pixels division.

4) *Result of experiment on right middle finger:* Table VII keeps the same conclusion made in the three previous experiments, the superiority of the recognition rates obtained with the classifiers based on the Jeffrey divergence and City-block is maintained. We see that the value of the most optimal recognition rate is 98.89% with city-block for the size 24x24 pixels. We are going to finish the experiments of this first part with the complement concerning the 11x22 block as before.

The block sizes of 11x22 pixels still ensure optimal recognition rates in Table VIII with a value of 98.89% for the 11x22 pixel block. This value is equal to the highest obtained in Table VII by the 24x24 pixel block with a value of 98.89%. In the end, we can conclude that dividing the sub-images into rectangular blocks can give results as optimal as square blocks.

TABLE VII. RECOGNITION RATE FOR RIGHT MIDDLE WITH TYPICAL BLOCKS

		Table Recognition rate RR (right middle)		
Block size	RR/MPT	Euclidian distance	Jeffrey divergence	City-Block
110x110	RR	83,23%	92,63%	90,71%
	MPT	0,950980 s	14,532302 s	1,141061 s
64x64	RR	93,03%	96,67%	96,67%
	MPT	1,019915 s	47,960191 s	1,817366 s
48x48	RR	94,54%	96,77%	97,37%
	MPT	1,665615 s	146,035030 s	4,346636 s
32x32	RR	97,27%	97,78%	98,48%
	MPT	1,935565 s	271,733796 s	6,986675 s
24x24	RR	97,07%	98,59%	98,89%
	MPT	2,396355 s	438,833175 s	10,932720 s
16x16	RR	96,77%	98,38%	98,18%
	MPT	3,809532 s	843,720436 s	21,210157 s

TABLE VIII. RECOGNITION RATE FOR RIGHT MIDDLE WITH RECTANGULAR BLOCK

		Table Recognition rate RR (right middle)		
Block size	RR/MPT	Euclidian distance	Jeffrey divergence	City-Block
11x22	RR	97,37%	98,48%	98,89%
	MPT	3,584845 s	868,403304 s	21,696460 s

C. Comparison and Analysis of Results

As we have already mentioned, we have set ourselves as objectives, the construction of a robust recognition system which offers a high recognition rate and a reduced computation time. The results obtained confirm our choice of distance-based classifiers with the method used for the extraction of local characteristics. Our choice thereafter to ensure the comparison of our mechanism with others in the literature will be based on the use of the city-block distance. The optimal results are in the following table:

TABLE IX. OPTIMAL OBTAINED RECOGNITION RATE

Table optimal Recognition rate				
Block size	Left index	Right index	Left middle	Right middle
11x22	98,48%	98,69%	98,89%	98,89%
16x16	98,18%	97,88%	99,29%	98,18%
24x24	98,08%	98,48%	98,89%	98,89%

We notice on the Table IX, that the block which shows the highest rates on average is the 11x22 block; we will take its results and compare them with those of the literature to remove the performance of the adopted mechanism.

TABLE X. COMPARATIVE STUDY

Table optimal Recognition rate				
Methods	Left index	Right index	Left middle	Right middle
PCA+LDA [22]	50.64 %	47.00%	51.08 %	54.68 %
CLPP [24]	86.58 %	86.43 %	85.89 %	86.16 %
OCLPP [24]	87.87 %	87.49 %	86.94 %	87.38 %
MSLBP [23]	93.80 %	94.70 %	92.20 %	94.80 %
LGBP [33]	94.14%	94.24%	97.27%	94.75%
LBP+DCT [32]	98.2%	98%	98.7%	97.1%
Our work	98,48%	98,69%	98,89%	98,89%

Table X shows that the preliminary results of the adopted process claim to be reliable, however there are still other aspects that we want to address to study and improve the support of our approach. This is what we will see in the next phase.

D. Global Evaluation of Proposed Approach

In this section, we will conduct our experiments to evaluate the proposed approach. These experiments consist in exploiting the sizes of the blocks, which have shown their performance previously, with a single finger knuckle print (24x24, 16x16, and 11x22). In this evaluation, we will use the approach with a fusion at the score level, with the city-block distance for the set of multi-instance combinations: left index with left middle (LI, LM) and right index with right middle (RI, RM). This choice is due to the fact that these combinations belong to the same hand, which facilitates the use and creation of sensors in a real recognition system. We will use the Cumulative Matching Characteristics (CMC) curves for each fusion case to measure the identification accuracy. CMC curves demonstrate the ability of a recognition system to identify a given user in a set of data. As the CMC

curve decreases, this represents an increasing amount of impostor images that are more similar than images of the required class, otherwise performance increases.

1) *Results of fusion left index and left middle results for block size 24x24 pixels:* In Fig. 7, we notice that the resulting curve for the fusion of the LI+LM instances is much higher than the other curves and it quickly tends towards 1. The higher recognition rate obtained with the approach equal to 99.90%, this rate is higher than the best rate obtained for studied systems with single instance, in this case left and right middle with 98.89%.

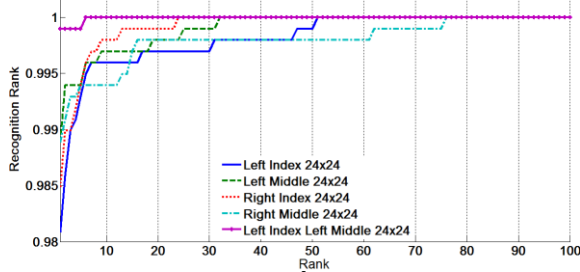


Fig. 7. CMC Curve for Fusion LI+LM with 24x24 Blocks.

a) *Results for block size 16x16 pixels:* In Fig. 8, we will report the same remark in the case of the block equal to 16x16. The recognition rate obtained with the approach is equal to 99.90%; this rate is higher than the best rate obtained for the systems studied previously.

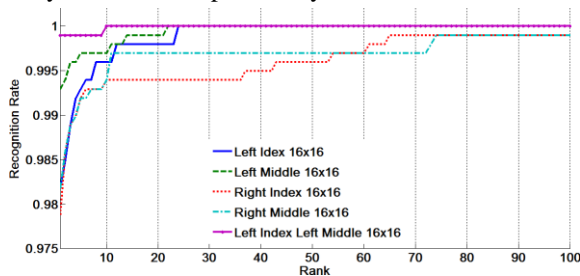


Fig. 8. CMC Curve for Fusion LI+LM with 16x16 Blocks.

b) *Results for block size 11x22 pixels:* In Fig. 9, we used the 11x22 pixel blocks and the resultant is a perfect curve with a score of 100% which outperforms all the curves.

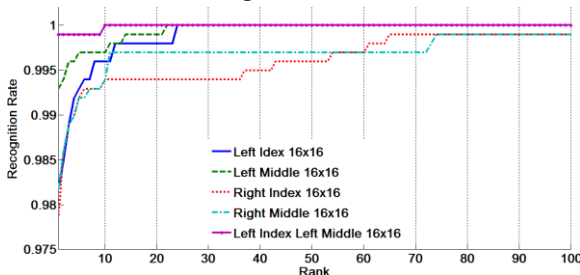


Fig. 9. CMC Curve for Fusion LI+LM with 11x22 Blocks.

2) *Results of fusion right index and right middle*

a) *Results for block size 24x24 pixels:* In Fig. 10, despite the recognition rate that the approach offers and which is equal = 99.80% for the fusion between Right Index and

Right Middle instances (RI, RM), but we notice the Right Index (system with single instance) curve overlaps with the (RI, RM) curve and it reaches values 1 well before the melting curve and this is due to the inter-class similarities.

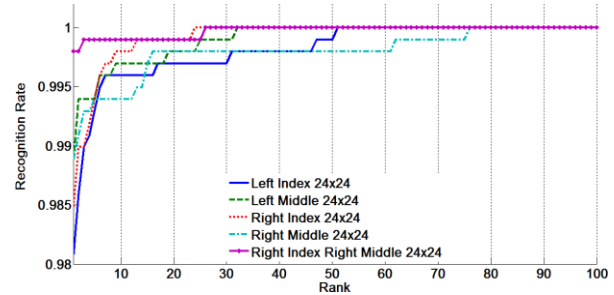


Fig. 10. CMC Curve for Fusion RI+RM with 24x24 Blocks.

b) *Results for block size 16x16 pixels:* In Fig. 11, despite the recognition rate offered by the approach and which is equal = 99.70% for the fusion between the instances Right Index and Right Middle (RI, RM) with the 16x16 blocks, but we notice that the curve (RI, RM) on the first 100 ranks it does not reach the values 1 and that it is exceeded by the Left Index curve and the Left Middle curve towards rank 24.

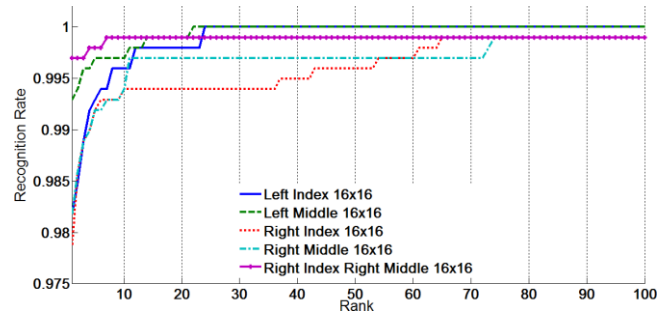


Fig. 11. CMC Curve for Fusion RI+RM with 16x16 Blocks.

c) *Results for block size 11x22 pixels:* In Fig. 12, we notice that the resulting curve for the fusion of the right index and right middle instances, in the case where the block size equal to 11x22 pixels is much higher than the other curves. The recognition rate obtained with the approach is equal to 99.70%, and reaches quickly the value 1 quickly before others curves.

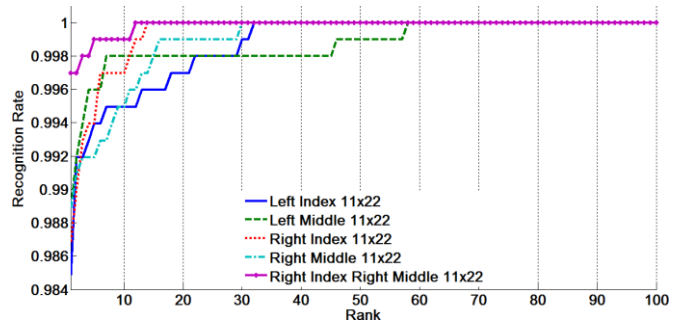


Fig. 12. CMC Curve for Fusion RI+RM with 11x22 Blocks.

3) *Comparison between fusion curves (LI, LM) and (RI, RM):* The results obtained show that the choices do not depend on the size of the block but also on its most suitable shape for

the subdivision of the source images. The performance of the results is shown in the Table XI. To confirm these hypotheses, we will obtain the CMC curves of all the mergers (LI, LM) and (RI, RM) with the 16x16, 24x24 and 11x22 blocks.

TABLE XI. RESULTS OF OUR APPROACH

	Recognition rate		
	Block size		
Instances	24x24	16x16	11x22
LI+LM	99,90%	99,90%	100%
RI+RM	99,80%	99,70%	99,70%

a) *Results for fusion(LI, LM):* In Fig. 13, The curve that represents the LI+LM fusion with the 11x22 block is a curve that surpasses the 2 other fusion curves with the 16x16 and 24x24 blocks. We notice that the fusion curve with the 24x24 blocks is more efficient and its convergence is faster towards the 1 than the 16x16 curve.

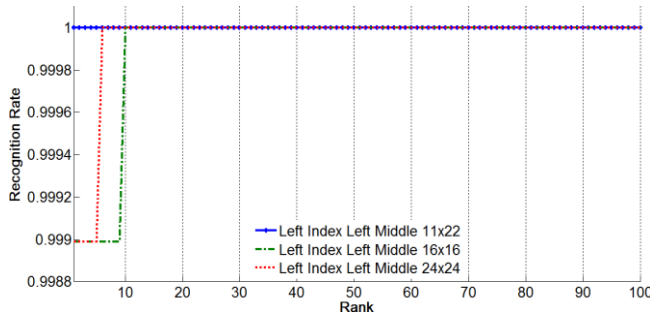


Fig. 13. CMC Curves for Fusion LI+LM.

b) *Results for fusion(RI, RM):* In Fig. 14, although the RI+RM fusion curve with the 24x24 block begins with a higher recognition rate compared to the RI+RM fusion curve with the 11x22 block, the latter tends towards ones more quickly than the curve 24x24 and 16x16.

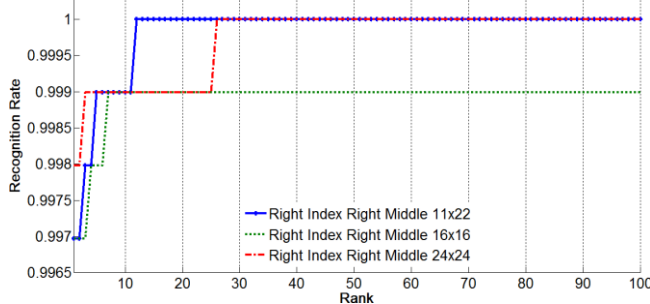


Fig. 14. CMC Curves for Fusion RI+RM.

All the experiments show very satisfactory results with the fusion approach adopted. The curves in Fig. 7, 8, 9, 10, 11 and 12 support these results. The introduction of the notion of the "block size \ image resolution" ratio in the experiments has shown its effectiveness and its ability to improve the results already obtained. The CMC curves Fig. 13 and Fig. 14 clearly demonstrate this improvement.

IV. CONCLUSIONS

In this paper, we evaluated the performance of the local CLBP descriptor, the influence of the block size parameter and its shape on the recognition rate. To improve efficiency and accuracy, we proposed an approach based on multi-instance fusion at the score level. The experimental results on the PolyU FKP reference database clearly show that the proposed approach increases the recognition rates (between 99.70% and 100%) and that it reduces the influence on the variance of the rates by taking charge of the adequate divider block according to the resolution of the image for the optimal construction of the histograms. Thus, we can conclude that this approach provides a noticeable performance improvement and can be usefully used for FKP recognition systems. The future works will focus on improving the security side of the recognition systems construction based on hand modalities. This improvement will aim to reduce the possibility of personal identity theft, while reducing the complexity of the mechanism to be built.

REFERENCES

- [1] G. E. Mardini, S. Massari, Body, biometrics and identity, Bioethics 22 (2008) p. 488–498.
- [2] Mahalakshmi B S and Sheela S V, "A Novel Feature Extraction for Complementing Authentication in Hand-based Biometric" International Journal of Advanced Computer Science and Applications(IJACSA), 12(9), 2021.
- [3] E. Marasco and A. Ross, "A survey on antispoofing schemes for fingerprint recognition systems," ACM Computing Surveys (CSUR), vol. 47, p. 28, 2015.
- [4] Zhao, T.; Liu, Y.; Huo, G.; Zhu, X. A deep learning iris recognition method based on capsule network architecture. IEEE Access 2019, 7, 49691–49701.
- [5] Rachida Tobji, Wu Di, Naem Ayoub and Samia Houassi, "Efficient Iris Pattern Recognition Method by using Adaptive Hamming Distance and 1D Log-Gabor Filter" International Journal of Advanced Computer Science and Applications(IJACSA), 9(11), 2018.
- [6] Zhang L, Shen Y, Li H Y, Lu J W, "3D palmprint identification using block-wise features and collaborative representation", IEEE Transactions on Pattern Analysis and Machine Intelligence, 37(8) :1730-1736, 2015.
- [7] Zhang D, Automated Biometrics: Technologies and Systems, Dordrecht: Kluwer Academic, 2000.
- [8] E. Yrk, E. Konukoglu, B. Sankur , and J. Darbon, "Shape-Based Hand Recognition," IEEE Transaction On. Image Processing, Vol. 15, No. 7, page 1803-1815, 2006.
- [9] D. N. Fernández, "Development of a hand pose recognition system on an embedded computer using Artificial Intelligence," 2019 IEEE XXVI International Conference on Electronics, Electrical Engineering and Computing (INTERCON), 2019, pp. 1-4.
- [10] .D. Zhang, W. Zuo, F. Yue, A comparative study of palmprint recognition algorithms, ACM Computing Surveys 44 (1) (2012) 2:1–37.
- [11] Jia W, Zhang B, Lu J T, Zhu Y H, Zhao Y, Zuo W M, Ling H B, Palmprint recognition based on complete direction representation. IEEE Transactions on Image Processing, 26(9) : 4483-4498, 2017.
- [12] Alonso-Fernandez, F., Fierrez, J., Ortega-Garcia, J., Gonzalez-Rodriguez, J., Fronthaler, H., Kollreider, K., Bigun, J.: A comparative study of fingerprint image quality estimation methods. IEEE Trans. on Information Forensics and Security 2(4), 734–743 (2007).
- [13] Nogueira, R.F., de Alencar Lotufo, R., and Machado, R.C.: 'Fingerprint liveness detection using convolutional neural networks', IEEE transactions on information forensics and security, 2016, 11, (6), pp. 1206-1213.

- [14] Z. Feng, B. Yang, Y. Chen, Y. Zheng, T. Xu, Y. Li, T. Xu, D. Zhu, Features extraction from hand images based on new detection operators, *Pattern Recognition* 44 (5) (2011) 1089–1105.
- [15] N. Duta, A survey of biometric technology based on hand shape, *Pattern Recognition* 42 (11) (2009) 2797–2806.
- [16] Tertychnyi, P., Ozcinar, C., and Anbarjafari, G.: ‘Low-quality fingerprint classification using deep neural network’, *IET Biometrics*, 2018, 7, (6), pp. 550–556.
- [17] Matsumoto, T., Matsumoto, H., Yamada, K. and Hoshino, S., Impact of artificial gummy fingers on finger-print systems, *Proc. SPIE, Optical Security and Counterfeit Deterrence Techniques IV*, vol. 4677, pp. 275–289, January 2002.
- [18] A. Kumar, C. Ravikanth, Personal authentication using finger knuckle surface, *IEEE Transactionson Information Forensics and Security* 4 (1) (2009) 98–109.
- [19] L. Zhang, L. Zhang, D. Zhang, and Z. Guo, “Phase congruency induced local features for finger-knuckle-print recognition,” *Pattern Recognition*, vol. 45, no. 7, pp. 2522–2531, 2012.
- [20] A. Kumar, C. Ravikanth, Personal authentication using finger knuckle surface, *IEEE Transactionson Information Forensics and Security* 4 (1) (2009) 98–109.
- [21] L. Zhang, L. Zhang, D. Zhang, and H.L. Zhu. Online finger-knuckle print verification for personal authentication. *Pattern Recognition*, 43(7):2560–2571, July 2010.
- [22] Z. S. Shariatmadar and K. Faez, “An efficient method for fingerknuckle-print recognition by using the information fusion at different levels,” in 2011 International Conference on Hand-Based Biometrics (ICHB), 2011, pp. 1–6.
- [23] W. El-Tarhouni, M. Shaikh, L. Boubchir, and A. Bouridane, “Multiscale shift local binary pattern based-descriptor for finger-knuckleprint recognition,” in *Microelectronics (ICM)*, 2014 26th International Conference on, pp. 184–187, Dec 2014.
- [24] X. Jing, W. Li, C. Lan, Y. Yao, X. Cheng, and L. Han, “Orthogonal complex locality preserving projections based on image space metric for finger-knuckle-print recognition,” in 2011 International Conference on Hand-Based Biometrics (ICHB), 2011, pp. 1–6.
- [25] Faisal Ahmed, Emam Hossain, A.S.M. Hossain Bari and ASM Shihavuddin, “Compound Local Binary Pattern (CLBP) for Robust Facial Expression Recognition,” *IEEE International Symposium on Computational Intelligence and Informatics*, pp.391-395, Budapest, Hungary, 2011.
- [26] PolyU finger knuckle print database (FKP) <http://www.comp.polyu.edu.hk/biometrics/FKP.htm>.
- [27] T. Ojala, M. Pietikainen and D. Harwood, A comparative study of texture measures with classification based on feature distributions, *Pattern Recognition*, vol. 29, 1996.
- [28]] Stan Z. Li, ChunShui Zhao, XiangXin Zhu, Zhen Lei, 2D+3D Face Recognition by Fusion at Both Feature and Decision Levels, In *Proceedings of IEEE International Workshop on Analysis and Modeling of Faces and Ges-tures*. Beijing. Oct 16, 2005.
- [29] AHMED, Faisal, HOSSAIN, Emam, BARI, A. S. M. H., et al. Compound local binary pattern (clbp) for rotation invariant texture classification. *International Journal of Computer Applications*, 2011, vol. 33, no 6, p. 5-10.
- [30] J. Inglada, Automatic recognition of man-made objects in high resolution optical remote sensing images by SVM classification of geometric image features, *ISPRS Journal of Photogrammetry and Remote Sensing*, vol.62, issue.3, pp.236-248, 2007.
- [31]] Giannis Lantzanakis, Zina Mitra, Nektarios Chrysoulakis, X-SVM: An Extension of C-SVM Algorithm for Classification of High-Resolution Satellite Imagery. *IEEE Trans. Geosci. Remote. Sens.* 59(5): 3805–3815 (2021).
- [32] M. Amraoui, M. El Aroussi, R. Saadane, M. Wahbi. Finger-knuckle-print recognition based on local and global feature sets. In *Journal of Theoretical and Applied Information Technology*, pp 054–060 Vol. 46. No. 1 – 2012.
- [33] Xiong, M., Yang,W., Sun, C.: Finger-knuckle-print recognition using lgbp. In: *International Symposium on Neural Networks*. ISSN (2011) 270–277.